Applied Surface Science 273 (2013) 491–495

Contents lists available at SciVerse ScienceDirect

Applied Surface Science

journal homepage: www.elsevier.com/locate/apsusc

Room-temperature preparation and properties of cadmium sulfide thin films by ion-beam sputtering deposition

Guang-Xing Liang[a,b], Ping Fan[a,b,*], Zhuang-Hao Zheng[a], Jing-Ting Luo[a,b], Dong-Ping Zhang[a,b], Chao-Ming Chen[a], Peng-Ju Cao[a]

[a] Institute of Thin Film Physics and Application, Shenzhen University, 518060, China
[b] Shenzhen Key Laboratory of Sensor Technology, Shenzhen University, 518060, China

ARTICLE INFO

Article history:
Received 29 January 2013
Received in revised form 9 February 2013
Accepted 16 February 2013
Available online 26 February 2013

Keywords:
CdS thin film
Ion-beam sputtering deposition
Microstructure
Optical and electrical properties

ABSTRACT

Deposition of cadmium sulfide (CdS) thin film on BK7 glass substrates has been prepared by a dry and in situ fabrication process with ion-beam sputtering deposition at room temperature. The structural, optical and electrical properties of CdS thin film were investigated. X-ray diffraction (XRD) analysis indicates the formation of polycrystalline CdS film with the mixed structure of cubic and hexagonal wurtzite phase. The Raman peaks are observed at 304 cm^{-1} and 606 cm^{-1}, and these peaks are identified as the first and second order LO optical phonons form of the CdS film. Energy dispersive X-ray Spectrometer (EDS) shows no other impurity elements, except Cd and S. The as-deposited film exhibits good transfer of the sintered target material with almost the same Cd/S ratio. Scan electron microscopy (SEM) and atomic force microscopy (AFM) reveal that the CdS thin film has a smooth surface and exhibited an obvious columnar growth indicating the *c*-axis preferred orientation. The detected room-mean-square (RMS) roughness by AFM is 0.76 nm. Optical transmission and absorption spectroscopy measurement reveal high absorption and energy band gap is of about 2.32 eV. The CdS thin film is of n-type conductivity and the resistivity is found to be in the order of 10^4 Ω cm. The CdS films annealed at 100 °C were demonstrated to be improvement in structural, electrical and optical properties.

1. Introduction

Of the II–VI semi-conducting materials, CdS is the leading candidate to be an excellent heterojunction partner for p-type cadmium telluride (CdTe) and p-type copper indium gallium diselenide (CIGS), due to its wide band gap (E_g = 2.42 eV), photoconductivity, and high electron affinity [1]. It is an interesting crystal material in the area of optoelectronic devices, photodetectors, semiconductor lasers, and nonlinear integrated optical devices. For the preparation of CdS thin films, various techniques have been employed, such as vacuum evaporation [2], closed–spaced sublimation (CSS) [3], magnetron sputtering [4], electrodeposition [5] and chemical bath deposition (CBD) [6–8]. Among these, chemical bath deposition (CBD) has become the favored route for its simpleness. However, it must be considered that CBD is not fast and gives a liquid waste that needs to be recycled, and the corresponding properties are easily influenced by contaminations in the nonvacuum process.

Little attention has been paid on the growth of CdS thin films by ion beam sputtering deposition (IBSD). Actually, IBSD has several advantages, such as excellent stoichiometry transfer of the target material, good uniformity and simple setup required for the film formation. In our latest work, for an innovative, all 'dry' and in situ fabrication process of ZnO/CdS/CIGS solar cells, IBSD has been successfully employed to deposited CIS absorber layers [9,10] and AZO window layers [11], respectively. For better solar cell efficient, the junction should be depositing at low temperature to avoid grain boundary diffusion. Moreover, the depletion should be in bulk of host material. Low-temperature-deposition CdS film provide the feasibility for reducing the thermally induced stress and minimizing interface diffusion between films and substrate, which is suitable for continuous and rapid roll-to-roll deposition process. The aim of this work is to explore the feasibility of CdS thin films prepared by IBSD at room temperature. The structural, surface morphology, electrical and optical properties of CdS thin films were investigated.

2. Experimental procedures

Fig. 1 shows the IBSD apparatus used for the CdS thin films preparation. The 110 mm × 110 mm × 3 mm square shaped targets

* Corresponding author at: Institute of Thin Film Physics and Application, Shenzhen University, 518060, China. Tel.: +86 755 653 6021; fax: +86 755 653 6021.
E-mail address: fanping308@126.com (P. Fan).

0169-4332/$ – see front matter © 2013 Elsevier B.V. All rights reserved.
http://dx.doi.org/10.1016/j.apsusc.2013.02.067

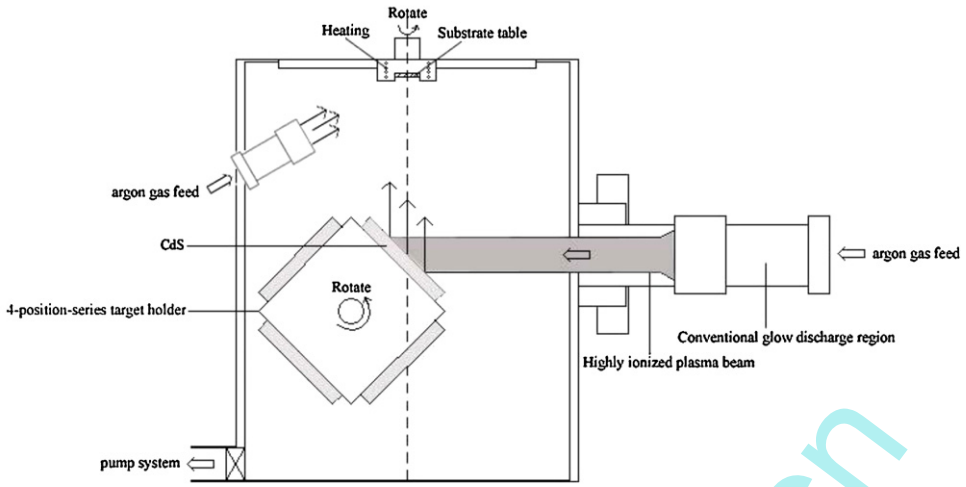

Fig. 1. Schematic diagram of the IBSD apparatus used for the CdS growth.

of CdS (99.99% purity) were fixed at target holder, as shown in Fig. 1. Prior to deposition, the substrates were ultrasonically cleaned in acetone and alcohol for 10 min, respectively. The vacuum chamber was evacuated to base pressure of 6.0×10^{-4} Pa. High-purity (99.99%) Ar of 6 sccm was introduced and deposition was carried out at working pressure of 6.0×10^{-2} Pa after presputtering for about 20 min to remove contaminants from the target. Using the IBSD technique, CdS thin films were deposited onto BK7 glass substrates at room temperature and after in situ (in the same vacuum with Ar of 6 sccm based on the pressure of 6.0×10^{-2} Pa) annealing at 100 °C for 1 h. More details on sample preparation are given in Table 1.

The crystallinity and crystal orientation of the films were determined by XRD technique (BRUKER-D8) with CuK_α radiation ($\lambda = 0.15406$ nm). Raman spectra measurement was performed using a Renishaw inVia Raman spectrometer with an Ar^+ laser excitation source (514.5 nm). The surface morphology of films was analyzed by a Hitachi SU-70 SEM and the composition was obtained by EDS attached to SEM. For SEM and EDS analyses, the acceleration voltage was chosen to be 5 kV. Due to the poor conductivity of CdS films, it needed to be coated with a thin layer of gold. CdS thin film thicknesses of as-deposited and annealed at 100 °C measured using the SEM cross-section were 461 and 457 ± 5 nm, respectively. The RMS surface roughness was characterized using an AFM (CSPM5500) in contact mode. Optical transmittance was obtained at room temperature by ultraviolet (UV)/visible (VIS)/near-infrared (NIR) spectrophotometer (Lambda 900, Perkin Elemer). Thermo electric power measurement (TEP) was carried out for determination of origin of conductivity. In the TEP measurements, the open circuit thermo voltage was generated by film sample when a temperature gradient was applied across a length of the sample and measured by Keithely 2400. The electrical sheet resistance R_s was determined using the four-point probe method, and the resistivity ρ was obtained using $\rho = R_s d$ where d is the film thickness.

Table 1
The ion-beam sputtering parameters used for preparing CdS thin films.

	Voltage (V)	Current (A)	Plasma energy (keV)
Screen	–	–	1.3
Anode	80	0.3	–
Acceleration	250	–	–
Cathode	8	12	–
Beam	–	0.02	–
Neutral	–	3.5	–

3. Results and discussion

The physical examination of CdS thin films prepared at room temperature by ion-beam sputtering deposition indicates that the films are uniform, transparent and yellowish in color. CdS films exhibit a good adhesion with no mechanical defects, such as cracks or peel-off. X-ray diffraction (XRD) patterns of as-deposited CdS films are shown in Fig. 2. It can be seen that the peaks at 26.42° and 42.46°, which can be assigned to the C(1 1 1) and C(1 1 0) planes of the cubic or H(0 0 2) and H(2 2 0) planes of the hexagonal structure of CdS, appear. It is generally acknowledged that the as-deposited film has a mixed cubic and hexagonal structure of CdS, because the positions of the peak C (1 1 1), C (1 1 0) of the cubic structure are similar to the peak H(0 0 2), H(2 2 0) of the more stable hexagonal structure, making difficult to illustrate the crystalline structure of the sample [12–16]. The highest reflection peak at $d = 3.37 \pm 0.01$ Å H(0 0 2)/C(1 1 1), which agrees well with the other reported value of 3.36 ± 0.01 Å [17]. The average crystalline size was estimated by resolving the highest intense peak using Scherrer's formula. It is found to be 108 ± 2 Å. After in situ annealed at 100 °C, the corresponding peak H(0 0 2)/C(1 1 1) is fixed at lower angle with 26.04° and the intensity becomes more intense and sharper. The observed increasement of H(0 0 2)/C(1 1 1) preferred orientation after annealed was attributed to the enhancement in surface diffusion of the absorbed species resulting in an improvement in

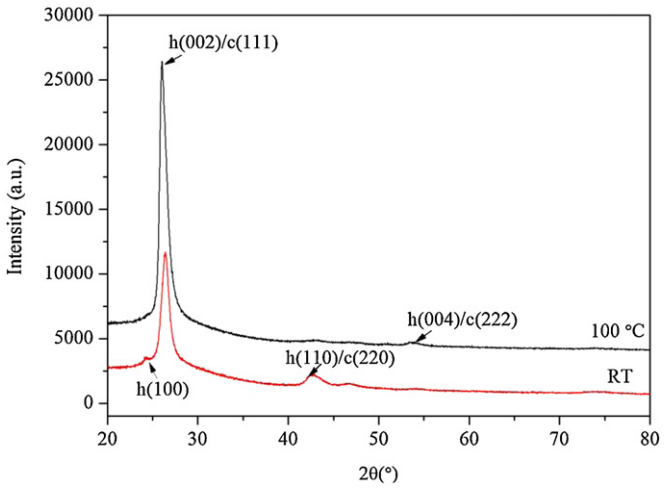

Fig. 2. XRD patterns of the as-deposited and annealed CdS films.

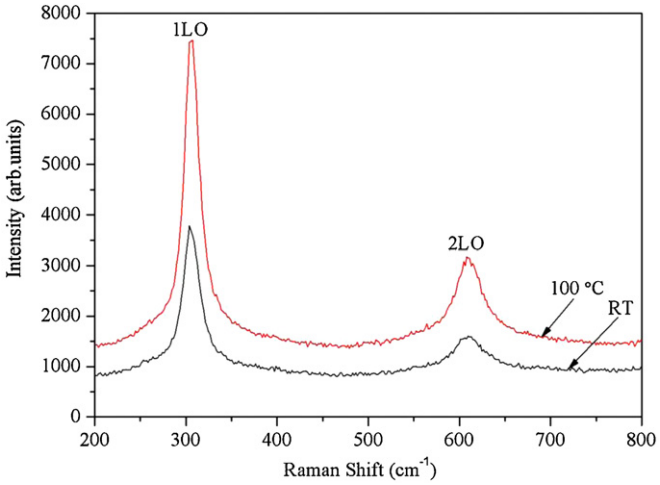

Fig. 3. Baseline corrected Raman spectra of the as-deposited and annealed CdS films.

crystallinity of CdS films and the calculated average crystalline size increases to 123 ± 2 Å.

Fig. 3 shows the Raman spectra of CdS thin films between 200 and 800 cm^{-1} after baseline correction. It is well known that Raman scattering spectra can give useful information about the crystalline of the film by evaluating the spectral peak position, intensity and spectral width of the Raman spectra. The Raman peaks of as-deposited film are observed at 304 cm^{-1} and 606 cm^{-1}, and these peaks are identified as 1LO and 2LO optical phonons form of CdS films. Thus, the prominent 1LO peak of as-deposited CdS film appears around 304 cm^{-1} while the 1LO phonon frequency for a bulk CdS was reported at 305 cm^{-1} [18], of which the slight peak shift is likely due to the confinement of phonons, optical as well as acoustic in the measured phonon spectra when the grain size falls to a few nanometers [19]. Comparing annealed film, it can be found that the intensity of the major peak at 304 cm^{-1} and 606 cm^{-1} increases obviously, which also suggests the enhancement in crystallinity. These results agree with the XRD data and conclusions.

Table 2
The composition of the CdS sintered target, as-deposited and annealed CdS thin films determined by EDS analysis.

Sample	Cd (at%) ±0.05	S (at%) ±0.05	Ratio Cd/S
Sintered target	58.46	41.54	1.40
As-deposited	57.47	42.53	1.35
Annealed	50.30	49.70	1.01

EDS was used to determine the chemical composition of the sintered target, as-deposited and annealed CdS thin films listed in Table 2. From Table 2, no other impurity elements can be found. It can be seem that the sintered target and as-deposited film with almost the same Cd/S ratio deviated from CdS stoichiometry. After annealed, the Cd/S is 1.01, which indicates that the elemental composition approached the stoichimetric composition ratio of 1:1 and also confirms the improved crystallinity. The surface morphology of CdS thin films is shown in Fig. 4 by SEM and Fig. 5 by AFM. The SEM and AFM images all reveal that the as-deposited CdS film has a smooth surface and the grain size increase after annealed. It also can be found that all the grain growth shows a certain trend and more obvious for the annealed films. From the cross-section images, the film grains exhibit an obvious columnar growth indicating the *c*-axis preferred orientation with good agreement to the XRD data and conclusions. The detected room-mean-square (RMS) roughness of as-deposited film is 0.76 ± 0.01 nm. After annealed, the grain size increases and the RMS roughness is found to be 2.93 ± 0.01 nm, which suggests that the diffusion and transfer ability of surface atoms are improved which leads to accelerated crystallization of CdS film and hence the enhancement of surface roughness.

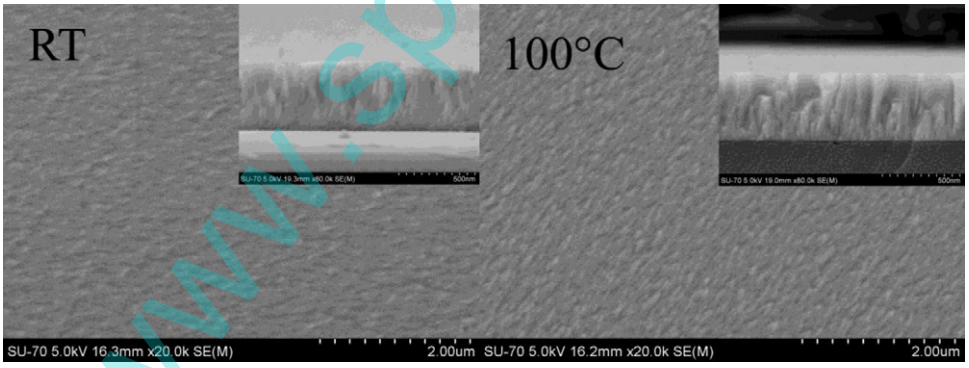

Fig. 4. SEM image of surface morphology and cross-section for as-deposited and annealed CdS films.

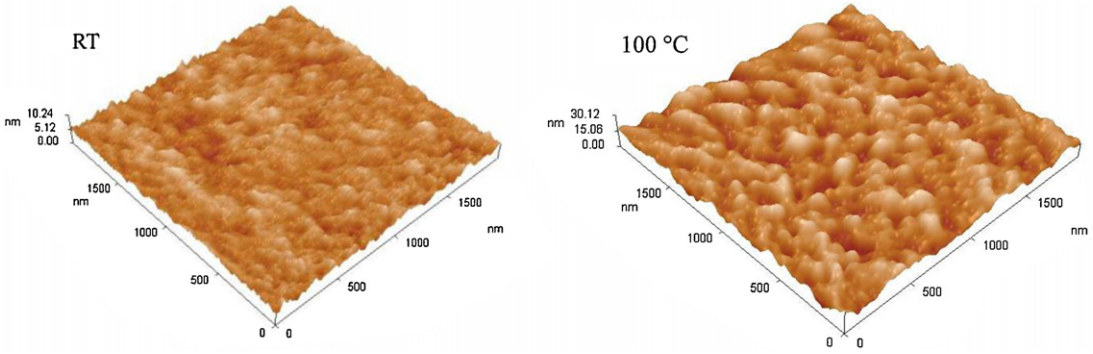

Fig. 5. AFM image of the as-deposited and annealed CdS films.

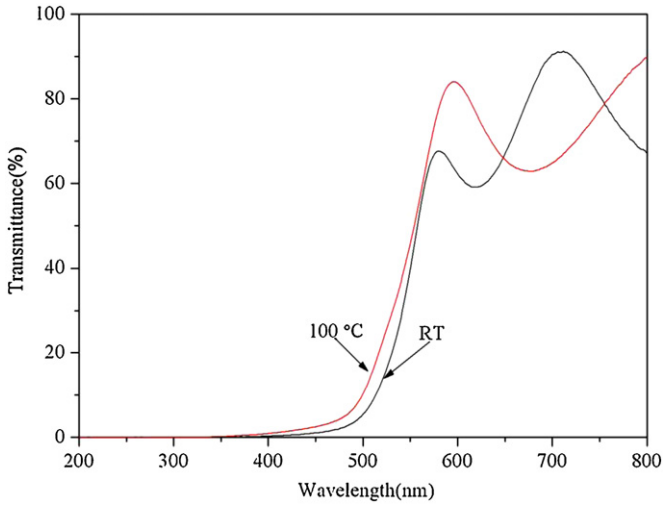

Fig. 6. Transmittance spectra of the as-deposited and annealed CdS films.

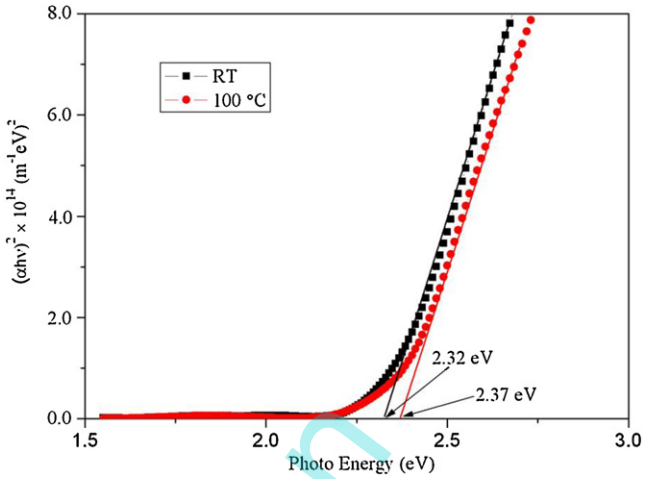

Fig. 8. Plot of $(\alpha h\tilde{o})^2$ vs. photo energy $h\tilde{o}$ for the as-deposited and annealed CdS films.

Fig. 6 shows the transmittance spectra as a function of wavelength in the visible spectrum for the as-deposited and annealed CdS films. The spectra show the usual interference pattern of a high refractive index film in the range of low absorption with a sharp absorption edge due to the direct transition of electrons from the valence band to the conduction, which indicates that the good crystallinity of CdS films is obtained. Fig. 7 shows the variation of coefficient of absorption with wavelength for CdS films. From Fig. 7, the prepared CdS films also reveal high absorption coefficient of about $10^5\,cm^{-1}$. The fundamental absorption, which corresponds to the electron excitation from valance band to conduction band, is usually used to determine the value of optical band gap (E_g). As a direct band gap semiconductor, CdS has an absorption coefficient ($\acute{a}$) obeying the following relation for high photon energies ($h\upsilon$) [20]:

$$\alpha h\upsilon = C(h\upsilon - E_g)^{1/2} \quad (1)$$

here C is a constant, υ the photon frequency and h the plank constant. As shown in Fig. 8, the optical energy band gap (E_g) of CdS films is determined from Eq. (1) by extrapolating the linear part of the spectrum $(\alpha h\upsilon)^2 = f(h\upsilon)$ to zero. It can be found that the calculated optical band gap of as-deposited and annealed films is 2.32 and 2.37 ± 0.04 eV, approaching the crystalline CdS (2.42 eV) and showing a 'red shift' of 0.10 and 0.05 eV. The existed defects really are the main influence. The CdS films could possess some impurities, including the donor impurity and the deep-level impurity. It is suggested that the deep-level impurity could exist under the conduction band, which shorten the gap between the conduction band bottom and the valence band top, and thus the Fermi level of CdS shift to lower value. Therefore, the band gap of CdS films is lower than that of CdS crystalline. Actually, there is error measurement in calculated the band gap and annealed film with 2.32 and 2.37 ± 0.04 eV, due to the fact that the band gap was obtained from extrapolating the straight portion of the $(\alpha h\upsilon)^2 vsf(h\upsilon)$ graph, on $h\upsilon$ axis at $\alpha = 0$. So in this method, the results may vary a little due to the uncertainties of choosing the portions for extrapolation [21].

Thermo-electric power is used for determination of conduction origin. TEP is negative for n-type semi-conducting materials i.e. charge carriers are negatively charge particle electrons. From the sign of terminal connected to cold end of the sample, one can decide the sign of the predominant charge carrier [22]. In our CdS films, the positive sign indicates the n-type of conduction mechanism and the measured film resistivity is found to be in the order of $10^4\,\Omega$ cm.

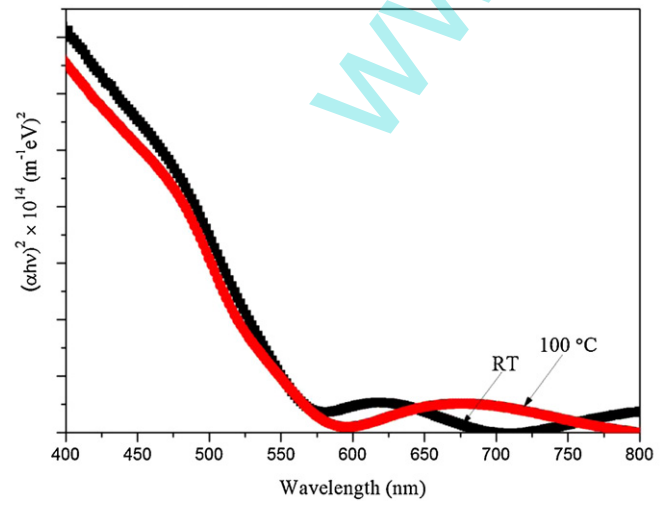

Fig. 7. Variation of coefficient of absorption α with wavelength λ for CdS films.

4. Conclusion

CdS thin film has been successfully deposited by ion-beam sputtering at room temperature. The structural, optical and electrical properties of CdS thin film were investigated. XRD analysis indicates the formation of polycrystalline CdS film with the mixed structure of cubic and hexagonal wurtzite phase. The Raman peaks are observed at $304\,cm^{-1}$ and $606\,cm^{-1}$, and these peaks are identified as the first and second order LO optical phonons form of the CdS film. EDS shows no other impurity elements, except Cd and S. The as-deposited film exhibits good transfer of the sintered target material with almost the same Cd/S ratio. SEM and AFM reveal that the CdS thin film has a smooth surface and exhibits an obvious columnar growth indicating the *c*-axis preferred orientation. The detected RMS roughness by AFM is 0.76 nm. Optical transmission and absorption spectroscopy measurement reveal high absorption and energy band gap is of about 2.32 eV. The CdS thin film is of n-type conductivity and the resistivity is found to be in the order of $10^4\,\Omega$ cm. The CdS films annealed at 100 °C was demonstrated to be improvement in structural, electrical and optical properties. In conclusion, high quality CdS thin films by IBSD can be obtained at low temperature. Thus, a simplified fabrication of functional devices in all 'dry' and in situ fabrication process can be achieved.

Acknowledgments

Supported by Basical Research Program of Shenzhen, China (JC201005250053A, JC201104210094A) and Natural Science Foundation of SZU (Grants No. 801 00035699).

References

[1] I. Oladeji, L. Chow, C. Ferekides, V. Viswanathan, Z. Zhao, Solar Energy Materials and Solar Cells 61 (2000) 203.
[2] D. Sreekantha Reddy, K. Narasimha Rao, K.R. Gunasekhar, Y. Dwarakanadha Reddy, P. Sreedhara Reddy, Journal of Alloys and Compounds 461 (2008) 34.
[3] V. Krishnakumar, K. Ramamurthi, A. Klein, W. Jaegermann, Thin Solid Films 517 (2009) 2558.
[4] B.S. Moon, J.H. Lee, H. Jung, Thin Solid Films 511 (2006) 299.
[5] J.M. Nel, H.L. Gaigher, F.D. Auret, Thin Solid Films 436 (2003) 186.
[6] O. Calzadilla, E. Hernández, E.M. Larramendi, F. Caballero-Briones, M. Zapata-Torres, M. Meléndez-Lira, A. Zapata-Navarro, Physica Status Solidi B 242 (9) (2005) 1933.
[7] J.K. Dongre, M. Ramrakhiani, Journal of Alloys and Compounds 487 (2009) 653.
[8] R. Mendoza-Perez, J. Sastre-Hernandez, G. Contreras-Puente, Solar Energy Materials and Solar Cells 93 (2009) 79.
[9] P. Fan, G.X. Liang, Z.H. Zheng, X.M. Cai, D.P. Zhang, Journal of Materials Science – Materials in Electronics 21 (2010) 897.
[10] P. Fan, G.X. Liang, Z.H. Zheng, X.M. Cai, D.P. Zhang, Thin Solid Films 519 (2011) 5348.
[11] G.X. Liang, P. Fan, X.M. Cai, D.P. Zhang, Z.H. Zheng, Journal of Electronic Materials 40 (2011) 267–273.
[12] K. Senthil, D. Mangalaraj, S.K. Narayandass, Applied Surface Science 169 (2001) 476.
[13] B.S. Moon, J.H. Lee, H. Jung, Thin Solid Films 511–512 (2006) 399–403.
[14] R.R. Bonn, N.C. Sandoval-Inda, F.J. Espinosa-Beltrán, Journal of Physics – Condensed Matter 9 (1997) 10051.
[15] O. Zelaya-Angel, J.J. Alvarado-Gil, R. Lozada-Morales, Applied Physics Letters 64 (1994) 291.
[16] J.R. Bakke, H.J. Jung, S.F. Bent, Chemistry of Materials 22 (2010) 4669.
[17] P.P. hankare, P.A. chate, D.J. Sathe, Solid State Sciences 11 (2009) 1227.
[18] B. Tell, T.C. Damen, S.P.S. Porto, Physical Review 144 (1966) 771.
[19] P. Chawla, S.P. Lochab, N. Singh, Journal of Alloys and Compounds 492 (2010) 662.
[20] J.I. Pankove, Optical Processes in Semiconductors, Dover Publications, New York, 1976.
[21] N.S. Das, P.K. Ghosh, M.K. Mitra, K.K. Chattopadhyay, Physica E 42 (2012) 2101.
[22] A.S. Khomane, Journal of Alloys and Compounds 496 (2010) 508.